J Fluoresc (2011) 21:1075–1082
DOI 10.1007/s10895-010-0780-4

ORIGINAL PAPER

The Limitations of Nonlinear Fluorescence Effect in Super Resolution Saturated Structured Illumination Microscopy System

Aviram Gur · Zeev Zalevsky · Vicente Micó · Javier García · Dror Fixler

Received: 8 August 2010 / Accepted: 25 November 2010 / Published online: 30 December 2010

Abstract Classically, optical systems are considered to have a fundamental resolution limit due to diffraction. Many strategies for improving both axial and lateral resolutions are based on a priori information about the input signal. These strategies lead to a numerical aperture improvement. However these are still limited by the wave nature of light. By using fluorescence technique one theoretically can reach unlimited resolution. The key point is to use the nonlinear dependence of the fluorescence emission rate on the intensity of the applied illumination. In this paper we present simulation as well as experimental results which show the advantage and the problems of using the nonlinear fluorescence effect in super resolution systems as well as discussing the nonlinear phenomena concerning the fluorescence process. The results show that the nonlinear fluorescence effect is accompanied by severe quenching, bleaching and saturation phenomena. As consequence, super resolution using saturated structured illumination method in living biological samples becomes severely restricted.

Keyword Fluorescence · Excitation power density · Photo damage · Super resolution · Saturation · Saturated structured illumination

A. Gur · Z. Zalevsky · D. Fixler (✉)
School of engineering, Bar Ilan University,
Ramat Gan 52900, Israel
e-mail: fixeled@mail.biu.ac.il

V. Micó · J. García
Departamento de Óptica, Universitat de Valencia,
C/Dr. Moliner, 50,
46100 Burjassot, Spain

Introduction

The resolution of an optical system is characterized by the finest detail that can be detected by that system. Classically, optical systems are considered to have a fundamental resolution limit due to diffraction [1] and super resolution methods are meant to enable detection of details beyond the classical diffraction limit. Super resolution is achieved by using a priori information about the input signal based on the classical works of Toraldo Di Francia and Lukosz which described an imaging system by the numbers of degrees of freedom it can transmit [2–6]. This a priori knowledge is used to encode the high spatial frequencies of the object and to transmit them through the band limited aperture. Later on to properly decode them and to generate a resolution enhanced image [7].

The process of encoding and decoding to produce enhanced resolution actually generates a synthetic aperture larger than the physical aperture of the imaging lens. The increase in the aperture can be used for resolution enhancement of spatial frequencies that are above $1/\lambda$ where λ is the optical wavelength (and in this case the super resolution approach synthetically decreases the effective F-number of the imaging lens) or to image sub wavelength features. In the later case it is essential that the encoding pattern will be positioned or generated in sufficient proximity to the inspected object such that the evanescent waves that are associated with the sub wavelength features will reach with sufficient energy to the encoding distribution. Obviously, the most appealing degree of freedom that can be used is the temporal one, owing to the high amount of available bandwidth for the cases in which the images are essentially static [7, 8].

However and as Abbe stated [1], the classical limit of resolution or super resolution is essentially limited by the

wave nature of light up to a maximum of half the illumination wavelength (depending on the illumination configuration). The main problem is that details having smaller dimensions produce evanescent rather than harmonic waves and they do not propagate in free space without a very strong attenuation.

To beat this resolution limitation, that is, to overcome the classical Abbe's resolution limit, several approaches have been proposed along the years [9–17]. For instance, confocal microscopy uses point illumination and a pinhole in an optically conjugate plane in front of the detector to eliminate out-of-focus information and extend resolution somewhat beyond the classical limit both axially and laterally [9]. Recently, two distinct conceptual strategies have overcome light's diffraction barrier, allowing the analysis of biological structures at the super resolution level. One strategy [10–12] was conceived in the context of laser-scanning microscopy and is designed to directly minimize the size of a scanned focal point, as in stimulated emission depletion (STED) fluorescence microscopy. Another method that we will mention in this paper suggests using saturated structured illumination microscopy (SSIM) [18].

Additional strategy for overcoming light's diffraction barrier uses photoswitchable molecules to resolve dense populations of molecules with super resolution. This approach employs stochastic activation of fluorescence to switch on individual photoactivatable molecules and then to image and to bleache them, temporally separating molecules that would otherwise be spatially indistinguishable [19, 20].

In this paper we deal with a derivation of the SSIM method. From the theoretical aspect using SSIM one may achieve resolution far beyond the diffraction limit by using the nonlinear dependence of the fluorescence emission rate on the illumination intensity [21, 22]. As consequence of the nonlinearity, the sample is illuminated by a pattern which contains sub lambda details. Such sub lambda illumination pattern demodulates the sub lambda features of the inspected sample and transmits those spatial frequencies through the system's aperture. Thus, by using optical microscope, fluorescence sample and nonlinear illumination effect, the system is theoretically capable of unlimited resolution.

But to our knowledge, no experimental demonstration considering biological samples has been published yet using the SSIM method. In other words, only simulations [21, 22] and experimental investigation of fluorescent beads [18] have been used to demonstrate the concept of nonlinear structured illumination wide field microscopy. In this paper we present simulations as well as experimental results showing the advantages and the problems associated with using fluorescence nonlinear effect in SSIM super resolution system. We will discuss the nonlinear phenomenon which is related to fluorescence process and conclude that in contrary to the initial theoretically expectation of unlimited resolution, the nonlinear effect is inhibited by a competition process involving quenching, bleaching and saturation. This is the reason why all the reported results published up-to-date present only simulation or samples of fluorescence beads (no experimental results based on biological samples).

The paper is organized as follows. The theory section presents the theory of nonlinear super resolution and simulates the advantages of using the nonlinearity in a super resolution system and describes the main non linear phenomenon in fluorescence. The materials and methods used in our work are described in the following section. Nonlinear fluorescence phenomena and experimental results are presented in the results section and the paper is concluded in the last section.

Theory

Theory of nonlinear super resolution

Let us first explain the theoretical background of our super resolving system while its sketch is shown in Fig. 1. The operation principle involves illuminating the sample with a set of high resolution patterns, each one with a slight lateral displacement. The same pattern, corrected by the system's magnification, serves to decode each frame. The final reconstructed image is obtained by averaging the captured low resolution images after being multiplied by the correct decoding pattern.

For simplicity, without loss of generality, we will assume a one dimensional process and a magnification of one. Let g(x) be the input object, s(x) the high resolution encoding pattern generated (or projected) on top of the sample plane, and s'(x) the decoding mask. We denote by ξ, the displacement of the encoding pattern in respect to the inspected object. The imaging system produces a low pass filtering which can be modeled by the impulse response

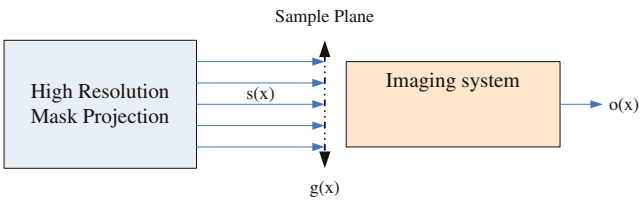

Fig. 1 Schematic sketch of basic system's setup

function denoted as h(x). Therefore, one single frame in the output plane will be

$$o_\xi(x) = [g(x)s(x-\xi)] \otimes h(x) = \int [g(x')s(x'-\xi)]h(x-x')dx' \quad (1)$$

where ⊗ denotes convolution. Then, the image is multiplied by the decoding pattern, displaced by the same amount as the encoding pattern while summing all the displacements. This yields the integrated image of:

$$o(x) = \int o_\xi(x)s'(x-\xi)d\xi = \int\int \{[g(x')s(x'-\xi)]h(x-x')\}s'(x-\xi)dx'd\xi \quad (2)$$

Rearranging the integration order and naming yields:

$$\gamma(x-x') = \int s(x'-\xi)s'(x-\xi)d\xi = \int s(v)s'(v+(x-x'))dv \quad (3)$$

Then we have

$$o(x) = \int g(x')h(x-x')\gamma(x-x')dx' = \int g(x')h'(x-x')dx' = g(x) \otimes h'(x) \quad (4)$$

Equation 4 expresses the final reconstructed image as a convolution with the impulse response associated with the full process, which is

$$h'(x) = h(x)\gamma(x) \quad (5)$$

The function $\gamma(x)$ is the correlation between the encoding and decoding masks. In the case that both coincide, it reduces to the autocorrelation of the encoding mask. When the encoding pattern is a random distribution, the autocorrelation will be a function which is highly concentrated at the origin. If, furthermore, the autocorrelation peak is narrow in comparison to the width of the impulse response of the imaging lens, then the autocorrelation expression can be approximated by:

$$h'(x) \approx h(x)\delta(x) = h(0)\delta(x) \quad (6)$$

Under these assumptions, a high resolution image is reconstructed according to Eq. 4 while the obtainable resolution limit will correspond to the width of $\gamma(x)$.

Note that although the expressions in Eqs. 2 and 3 assumes continues integration along the displacement parameter ξ or v, in order to obtain the super resolved reconstruction a discrete set of images can be sufficient. Actually the number of discrete images should correspond to the resolution improvement factor that we aim to obtain, i.e. the ratio between h(x) the impulse response of the existing imaging system and the desirable narrow impulse response h'(x). To show this using matrix representation is more suitable.

Assuming that $\overline{g}$ is a vector having dimensions of N X 1 and which is representing the field of view limited input object while each sample of this vector corresponds to the high spatial resolution available in the input object. The input field of view has N spatial samples. Assuming that H is the blurring matrix which has dimensions of N X N. After the multiplication of $\overline{g}$ by H a reduced resolution vector is obtained. We assume that S_ξ is the encoding matrix which is a diagonal matrix with the components of the displaced s(x), i.e. s(x- ξ) along its diagonal. Thus, it has the dimensions of N X N as well. We will also assume that M is the resolution improvement factor we wish to obtain. Therefore the output vector $\overline{o}_\xi$ to be obtained according to Eq. 1 for a given displacement can be described as:

$$\overline{o}_\xi = \left(\overline{g}^t S_\xi\right) H \quad (7)$$

The reconstructed output vector after the M summations will be:

$$\overline{o} = \sum_{\xi=\xi_1}^{\xi_M} \overline{o}_\xi S_\xi = \overline{g}^t \left(\sum_{\xi=\xi_1}^{\xi_M} S_\xi H S_\xi \right) \quad (8)$$

Note that if each element along the diagonal of S_ξ is different, i.e. the expected resolution of the encoding/decoding patterns matches the original resolution of the object vector, then the matrix product in the brackets will become a matrix having number of non zero rows (with values around its diagonal) of N/M. For M = N the matrix products in the brackets will become a diagonal matrix. Therefore the final reconstructed resolution will correspond to N/M times the resolution of the original inspected object.

The above describes a regular super resolved imaging which contains no sub lambda features as well as a sub lambda system but in the second case the projected pattern must also contain sub lambda features which can be achieved mainly by using nonlinear fluorescence effects.

When nonlinearities are present in the process, higher order terms appear in the Fourier transform. The positions of the resulting peaks of the emitted pattern now lie beyond the limiting spatial frequency given by the optical transfer function (OTF) of the imaging system. Although it permits only the detection of rather low spatial frequencies of the emission pattern, the attachment of the Fourier-transformed object to these high frequency peaks allows the detection of object's spatial frequencies which are beyond the limits obtained by linear pattern excitation. That is, in the nonlinear case higher-spatial-frequency information is

shifted into the range of spatial frequencies that is detectable by the system, to a degree determined by the order of the respective nonlinear term. In theory, this circumstance permits the detection of object's information at arbitrarily high spatial frequencies and therefore with arbitrary high resolution, although in practice the achievable resolution will be limited by the signal-to-noise ratio (SNR) of the raw data.

Simulations of the theory of nonlinear super resolution

In order to prove the above mentioned concept a simulation of the system that is shown in Fig. 1 was designed. The virtual microscope was demonstrated with a Point Spread Function (PSF) that uses numerical aperture of NA=1 and optical wavelength of λ=532 nm. In Fig. 2 one can see the cross section of an absolute square of a simulated PSF that corresponds to Rayleigh resolution limit (=1.22λ/2NA) of 325 nm. Figure 3 presents the cross section of the absolute square of the high resolution encoding mask (s(x)) which is generated due to the nonlinear emission of a projected speckle pattern [23] that was diffused from a diffuser being illuminated by a Gaussian beam. One can see that some lobes of the speckles are smaller than half of the simulated wavelength ($\lambda/2 \sim 250nm$) which means that higher spatial frequencies are encoded and thus can go through the band limited imaging system.

Figure 4 shows the simulation results of a virtual microscope. High input resolution image of an USAF resolution target can be seen in Fig. 4(a). The full size of the resolution target is 20 μm×20 μm and it contains features larger as well as smaller than the optical wavelength. Figure 4(b) shows the results of "observing" the high resolution target through the virtual microscope using the PSF presented in Fig. 2. Such observation is

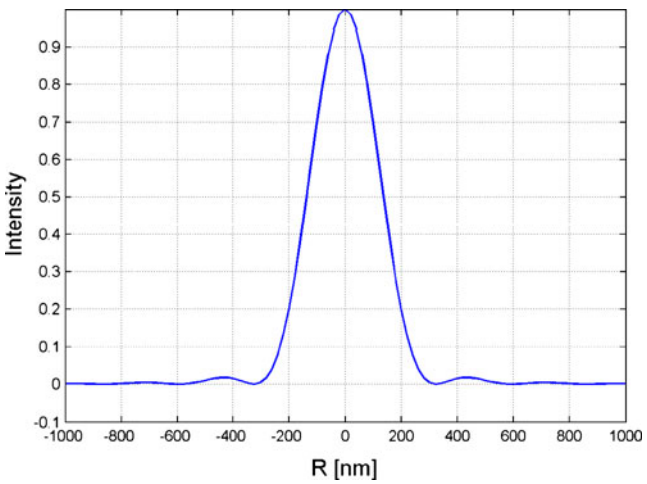

Fig. 2 Absolute square simulated PSF with NA=1, λ=532 nm

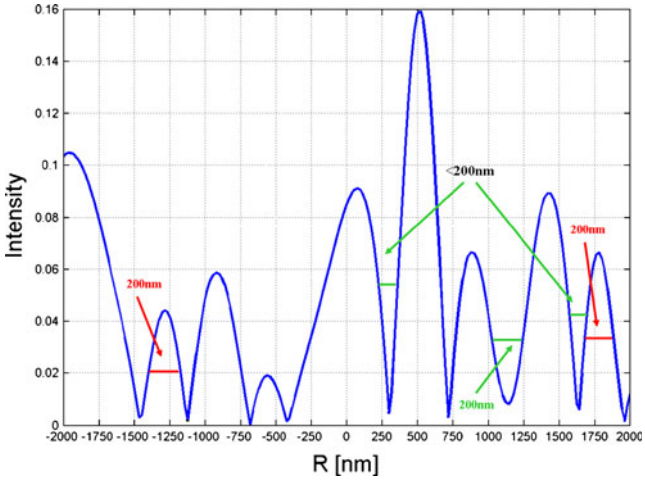

Fig. 3 Absolute square simulated mask of non linear speckle pattern which contains sub-wavelength features. As can seen at the figure spatial features of 200 nm and smaller are visible

corresponding to the relation of: $I_{out} = I_{in} \otimes PSF$ where I_{in} is the high resolution intensity of the inspected object, I_{out} is the intensity of the output image and PSF is the point spread function causing to the reduction of the imaging resolution. In Fig. 4(c) the super resolved image after applying the proposed method is presented. One can easily distinguish between sub-wavelength features which cannot be observed through a conventional system.

In order to get nonlinear fluorescence phenomena, high illumination intensity is needed. Applying such a single line (or narrowband) light source is not simple. Moreover, such high power might lead to effects that will change the illuminated fluorescent marker, not to mention that is may affect the sample itself. However, unfortunately experience shows that such undesired effects occur even at much lower illuminating intensities [24, 25].

Therefore, in principle, the sub lambda super resolving effect can be obtained. Nevertheless, one needs to carefully analyze the different (and mutually competing) nonlinear phenomena occurring in the fluorophore.

Non linear phenomenon in fluorescence

The heart of our suggested method is to get non-linear dependence between the fluoresce emitted light and the excitation intensity. However, while dealing with non-linear range of fluorescence other phenomenon can affect the fluorescence process. For example, photosaturation is an effect in which, beyond certain excitation intensity, no increase in the fluorescence intensity is observed. This phenomenon was already described as a concept for resolution improvement [21, 22]. It was also part of the work done by Gustafsson [18] which used this non linearity of the

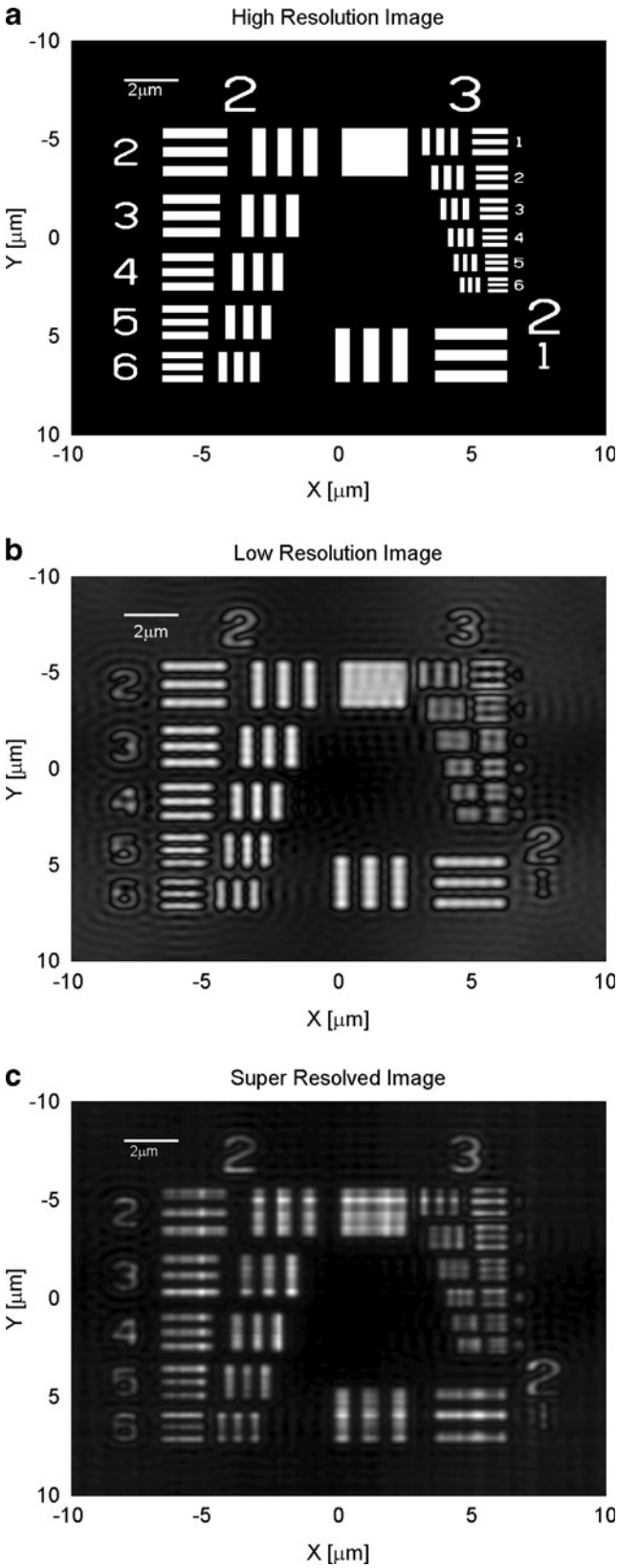

Fig. 4 Simulation results of the proposed method. **a** High resolution target image; **b** Observing the target through the virtual microscope; **c** Super resolved image

fluorescent layer in order to extract sub wavelength features by illuminating the sample with periodic patterns. While using structured-illumination microscopy, as Gustafsson described, the number of photons that each molecule can emit before being destroyed is smaller under saturating conditions compared with normal illumination intensities. At the same time, the number of detected photons required for a given signal-to-noise-ratio is greatly increased compared with a single conventional image.

Another process that affects the fluorescence process is photobleaching (Q_b). This effect happens when fluorescent molecules enter a state in which they are non-fluorescent. This phenomenon is non-linear, meaning that the final chemical bleached product is not linearly related to the illumination power density [26, 27].

Photobleaching is usually the main problem for time-course measurements (movies). Photobleaching prevents measuring nonlinear florescence process. These are competing processes.

The present study deals with the limitations of using fluorescence process in the non-linear range while photo-damage and photobiostimulation might affect the measured elements as reported in Refs. [28, 29] and even to damage the biological sample [30].

Materials & methods

The work presented in this paper combines the proposed super resolved configuration suited to an inverted as well as upright microscope with an obliquely illumination of the inspected biological solutions and cells with blue and green laser at wavelength range of 405–532 nm.

In the experiment we have used Olympus IX81 and BX51 and objectives of UPlanSApo 10×/0.40 and 60×/1.0. The biological samples were illuminated with blue and green lasers. Images were captured using Pixelink PL-A741-E camera (PixeLINK, Ottawa, ON) having pixel size of 7 μm×7 μm which was connected to the microscope. The output of the Pixelink camera was connected to a computer which was capturing video frames using the manufacturer's software. The captured video was analyzed by MATLAB (The MathWorks, Natick, MA) software.

Excitation

A 5 W (all lines) argon laser (Spectra Physics and Coherent) and green doubled Nd:YAG laser at wavelength of 532 nm have been used as the source of excitation. The excitation wavelengths in most of these investigations were 488 nm and 532 nm, with intensity at the interrogation point of hundreds of milliWatts.

Emission

In most of the investigations the fluorescent emission was measured either through a long-wavelength cut-off filter (λ>500 nm for the blue laser and λ>580 for the green laser) or a broadband interference filter (500–560 nm, 580-630 nm) to collect most of the fluorescence emission. All filters are from Chroma (Chroma Technology, Brattleboro, VT).

Cell line

U937 cells were maintained in RPMI-1640 medium supplemented with 10% heat-inactivated fetal calf serum, 100 U/mL penicillin, 100 μg/mL streptomycin, 2% glutamine, 2% sodium pyruvate and 2% HEPES (complete medium). All the materials were obtained from Biological Industries (Kibbutz Beit Haemek, Israel). Cells were maintained in completely humidified air with 5% CO_2 at 37°C. Before use, the exponentially grown cells were collected, washed and re-suspended at a concentration of 2×10^6 cells/mL.

Cell labeling and dyes

Cells, at a concentration of 2×10^6 cells/mL in PBS, stained for 30 min at 37°C, 5% CO_2, with 13 μM Rhodamine 123 (RH123), and then double washed in PBS and re-suspended at a concentration of 2×10^6 cells/mL in PBS. 10 μl were loaded onto the microscope slide.

As fluorescence dyes additional to RH123 we used Nonyl Acridine Orange and Carboxy SNARF-1 (all from Sigma, St. Louis, MO, USA) in order to have different types of dyes to test the investigated phenomenon.

Experimental results

Photosaturation

Photosaturation process was the main technique used in the work of Gustafsson introducing the SSIM method [18]. In his paper he demonstrated non linearity of fluorescent layer in order to extract sub wavelength features by illuminating the sample with a periodic pattern. Unfortunately he did not measure living biological samples while targeting to a fluorescent object. In order to illuminate the target with fluorescence light, much higher excitation intensity is needed.

We performed experiments using green laser (λ= 532 nm) with maximal output power of 400 mW and different fluorescence dyes (free Acridine Orange and Carboxy SNARF-1 in pH=6) in different concentrations. In all the results non linearity was not reached as can be seen by the solid line curve of Fig. 5. Although we did not get the non-linear effect we start getting photobleaching.

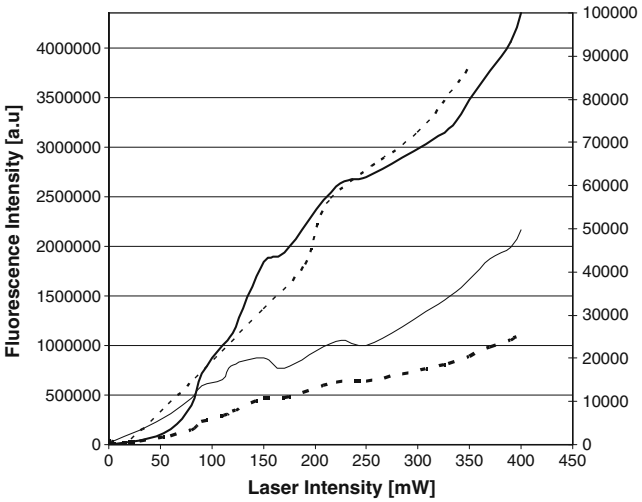

Fig. 5 Fluorescence intensity of Acridine Orange (*solid thick line*), Carboxy SNARF-1 (*solid thin line*), U937 cells stained with RH123 (*dashed line*) and Acridine Orange at parallel directions (*thin dashed line*. The values are presenting at the secondary Y axis) for different laser's intensities

The fluorescence intensity decrease in 35±8% during 3 min of continues exposure.

Additional linearity tests were performed on fluorescent beads (6.5 mm diameter, Polyscience, Inc., Warrington, PA, USA) and also for this type of samples the linear dependence was preserved. Those results are in agreement with measurements that tested the dependence of the fluorescence polarization on the excitation level [30].

Photosaturation in parallel direction

When fluorescent markers in biological sample, like cells or beads, are excited by polarized light, molecules whose dipole moment of absorption is parallel to the direction of the exciting field are predominantly excited while those in other directions absorb less. When the photosaturation process takes place, at the first stage, it leads to an absorption saturation of the parallel dipoles while those at an angle to the exciting field continue to increase their emission with the increasing excitation intensity. Apparently, this causes a decrease in the measured polarization. This is a possible explanation of the findings of Keene and Hodgson [31] and Pinkel et al. [32], which showed that the polarization of fluorescent beads decreases when increasing the excitation energy.

We preformed this kind of measurements while using free Acridine Orange and Carboxy SNARF-1 in pH=6 and measuring the fluorescence intensity using two polarizer that were positioned in parallel to each other, along the optical path of excitation as well as emission. The results for Acridine Orange are presented in Table 1 and at Fig. 5 thin dashed line. As it can be seen the linear dependence of

Table 1 Fluorescence intensity of Acridine Orange at parallel directions versus the power of the excitation laser. It can be seen that linear dependence exists for the entire range of applied intensities

Laser Power [m Watt]	Fluorescence intensity [arbitrary units]
0.6	963±15
22	1,166±150
150	31,454±220
190	41,685±113
215	56,930±200
300	72,176±205
350	87,421±180

the fluorescence intensity still exists even at excitation power of 350 mW and while measuring only the parallel direction of the electromagnetic wave. Similar results were obtained for Carboxy SNARF-1.

Photobleaching

Photobleaching effects were examined on tens of human U937 cells that were stained with RH123 dye. The results can be seen in Fig. 5 where the dashed line presents similarity to the fluorescence dye experiments that were presented in section 4.1. While starting the measurement from high intensity of 400 mW and going down to few mili-Watts we obtained the results being presented in Fig. 5. However, when starting the measurement from the opposite direction, meaning from low intensity level (few mili-Watts) and going up to the higher intensity of 400 mW, we obtained that during 45 s of exposure the fluorescence intensity decreased by 42±12%. These results are presented in Fig. 6. Figure 6 presents the images of U937 cells before and after the 400 mW exposure. The images, that were done by sensitive fluorescence microscope, show us that the RH123 dye decreased, from the beginning of the measurement (t=0 Fig. 6 middle images), during 45 s (Fig. 6 right images) by more than 40%. The meaning is that in normal leaving cells that are stained by RH123 the dye exists in the entire cell, but 400 mW illumination bleach the fluoresce dye.

Control measurement was done on fluorescent beads (6.5 mm diameter, Polyscience, Inc., Warrington, PA, USA) that were used in section 4.1 and the obtained results show that there is no trace of photobleaching in the excitation power range of 50 mW to 600 mW. The meaning of this result is that even at 600 mW of CW laser, nonlinear effects are still not shown while those high power density already affects the biological sample.

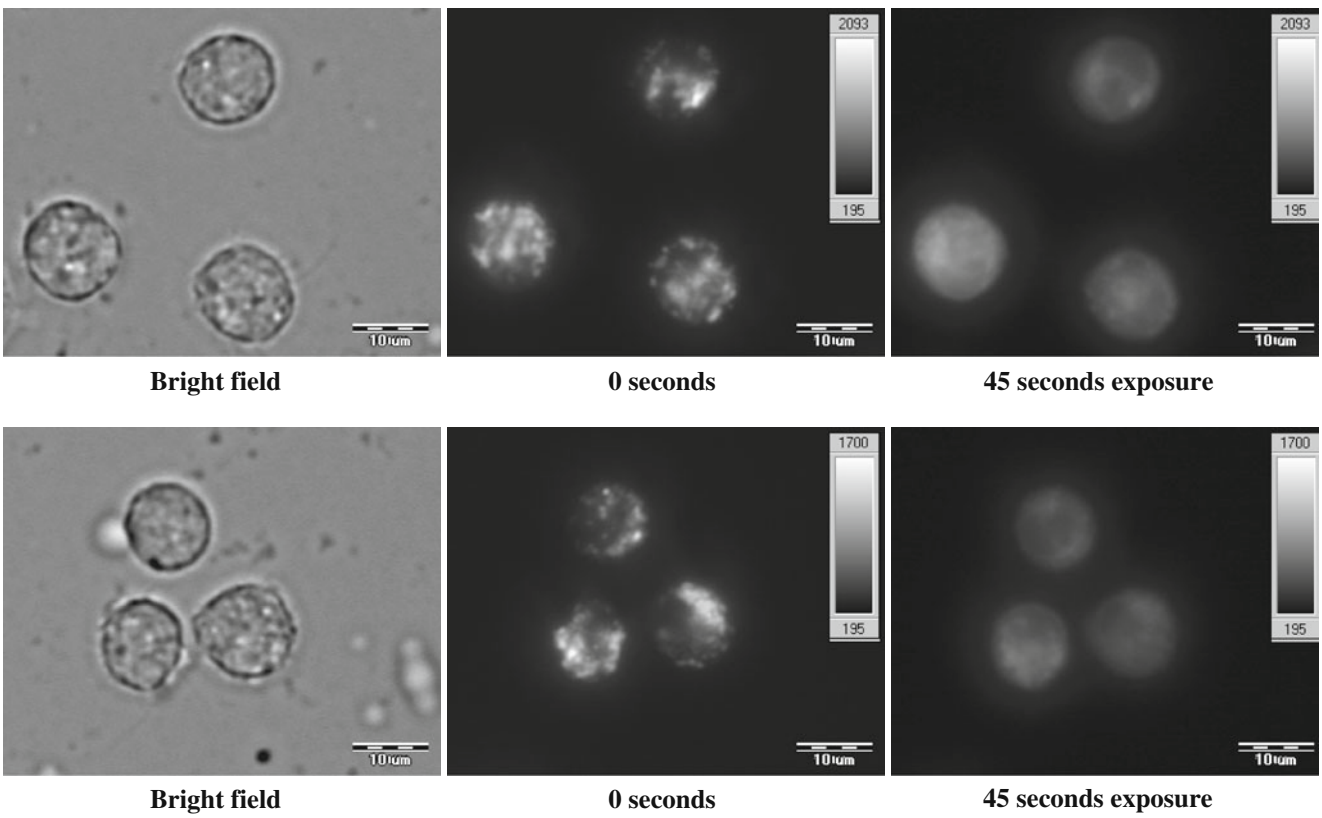

Fig. 6 U937 cells as seen at bright field microscopy (left images of both panels) stained with 25 μM Rh123 immediately after the first exposure by 400 mW (middle images of both panels) and after 45 s (right images of both panels)

Conclusions

In this paper we have studied the limitations involved in applying nonlinear fluorescence effect to sub lambda super resolution microscopy in biological samples. Moreover, we have proposed a technique based on speckle pattern projection and fluorescence nonlinearities to achieve theoretical unlimited spatial resolution. In order to get this, nonlinear dependence of the fluorescence emission rate on the illumination intensity is used. In theory as well as in simulations in the nonlinear case higher-spatial-frequency information is shifted into the low range of spatial frequencies that may be detectable by the imaging system. As proved in the theory and in the simulations, the nonlinear case permits the detection of object's information at arbitrarily high spatial frequencies and therefore with unlimited resolution.

Unfortunately it is not easy to demonstrate nonlinear characteristics while using CW laser with standard biological samples such as proposed by the SSIM method. The intensity that is required in order to obtain good fluorescence measurements is quit high as calculated in this paper. Even trying to perform the measurement in lower intensity levels generates a competitive reaction to photobleaching which affects the system and in case of living cell may harm their natural activity.

Theoretically speaking photobleaching in cells may be avoided by using diamond nanocrystals containing nitrogen-vacancy color centers. However, it is not applicable for most of the biological applications that attempt measuring living cells in vivo or in culture. To the same conclusion but from different point-of-view arrived recently Lang and Rizzoli [33]. Although highly photo-stable fluorescent labels do exist, they are not common for living biological samples and saturated structured illumination cannot be used there.

References

1. Abbe E (1873) Beitrage zur theorie des mikroskops und der mikroskopischen wahrnehmung. Arch Mikrosk Anat 9:413–468
2. Toraldo Di Francia G (1955) Resolving power and information. J Opt Soc Am 45:497–501
3. Toraldo Di Francia G (1969) Degrees of freedom of an image. J Opt Soc Am 59:799–804
4. Lukosz W (1967) Optical systems with resolving powers exceeding the classical limits. J Opt Soc Am 56:1463–1472
5. Lukosz W (1967) Optical systems with resolving powers exceeding the classical limits II. J Opt Soc Am 57:932–940
6. Cox IJ, Sheppard JR (1986) Information capacity and resolution in an optical system. J Opt Soc Am A 3:1152–1158
7. Zalevsky Z, Mendlovic D (2002) *Optical super resolution*. Springer.
8. Shemer A et al (1999) Superresolving optical system with time multiplexing and computer decoding. Appl Opt 38:7245–7251
9. Semwogerere D, Weeks ER (2005) *Confocal microscopy*, encyclopedia of biomaterials and biomedical engineering. Taylor & Francis
10. Hell SW, Kroug M (1995) Ground-state-depletion fluorescence microscopy: a concept for breaking the diffraction resolution limit. Appl Phys B 60:495–497
11. Schönle A, Hänninen PE, Hell SW (1999) Nonlinear fluorescence through intermolecular energy transfer and resolution increase in fluorescence microscopy. Ann Phys (Leipzig) 8:115–133
12. Schönle A, Hell SW (1999) Far-field fluorescence microscopy with repetitive excitation. Eur Phys J D 6:283–290
13. Heintzmann R, Cremer C (1999) Laterally modulated excitation microscopy: improvement of resolution by using a diffraction grating. Proc SPIE 3568:185–195
14. Frohn JT, Knapp HF, Stemmer A (2000) True optical resolution beyond the Rayleigh limit achieved by standing wave illumination. Proc Natl Acad Sci U S A 97:7232–7236
15. Frohn JT, Knapp HF, Stemmer A (2001) Three-dimensional resolution enhancement in fluorescence microscopy by harmonic excitation. Opt Lett 26:828–830
16. Gustafsson MGL (2000) Surpassing the lateral resolution limit by a factor of two using structured illumination microscopy. J Microsc 198:82–87
17. Gustafsson MGL et al (2008) Three-dimensional resolution doubling in wide-field fluorescence microscopy by structured illumination. Biophys J 94:4957–4970
18. Gustafsson MGL (2005) Nonlinear structured-illumination microscopy: wide-field fluorescence imaging with theoretically unlimited resolution. Proc Natl Acad Sci USA 102:13081–13086
19. Betzig E et al (2006) Imaging intracellular fluorescent proteins at nanometer resolution. Science 313:1642–1645
20. Rust MJ, Bates M, Zhuang X (2006) Sub-diffraction-limit imaging by stochastic optical reconstruction microscopy (STORM). Nat Meth 3:793–795
21. Heintzmann R, Jovin TM, Cremer C (2002) Saturated patterned excitation microscopy - a concept for optical resolution improvement. J Opt Soc Am A 19:1599–1609
22. Heintzmann R (2003) Saturated patterned excitation microscopy with two-dimensional excitation patterns. Micron 34:283–291
23. Garcia J, Zalevsky Z, Fixler D (2005) Synthetic aperture super resolution by speckle pattern projection. Opt Exp 13:6073–6078
24. Lindmo T, Steen HB (1977) Flow cytometric measurement of the polarization of fluorescence from intracellular fluorescein in mammalian cells. Biophys J 18:173–187
25. Rotman B, Papermaster BW (1966) Membrane properties of living mammalian cells as studied by enzymatic hydrolysis of fluorogenic esters. Proc Natl Acad Sci 55:134–141
26. Bloom JA, Webb WW (1984) Photodamage to intact erythrocyte membranes at high laser intensities: methods of assay and suppression. J Histochem Cytochem 32(6):608–616
27. Lubart R et al (1993) Light effect on fibroblast proliferation. Laser Therapy 5:55–57
28. Sheetz MP, Koppel DE (1979) Membrane damage caused by irradiation of fluorescent concanavalin A. Proc Natl Acad Sci USA 76:3314–3317
29. Shapiro HM (1983) Apparatus and method for killing unwanted cells, *United States Patent* 4395397
30. Deutsch M et al (2002) Fluorescence polarization as a functional parameter in monitoring living cells: theory and practice. J Fluoresc 12(1):25–44
31. Keene JP, Hodgson BW (1980) A fluorescence polarization flow cytometer. Cytometry 1(2):118–126
32. Pinkel D et al (1978) Fluorescence polarimeter for flow cytometry. Rev Sci Instrum 49(7):905–912
33. Lang T, Rizzoli SO (2010) Membrane protein clusters at nanoscale resolution: more than pretty pictures. Physiology 25:116–124